Vol. 45, No. 2 (2023) 340-350, DOI: 10.24874/ti.1460.03.23.05

Tribology in Industry

www.tribology.rs

RESEARCH

Elastic-Plastic Properties of hard Cr-Based Nitride Coatings Deposited at Temperatures Below 200°C

Vassiliy Chitanov[a], Ekaterina Zlatareva[a,*], Lilyana Kolaklieva[a], Roumen Kakanakov[a], Tetiana Cholakova[a], Stefan Kolchev[a], Chavdar Pashinski[a,b]

[a]*Central Laboratory of Applied Physics, Bulgarian Academy of Sciences, Bld. Sankt Petersburg, 61, 4000 Plovdiv, Bulgaria,*
[b]*Department of Mechanics, Technical University - Sofia, Br. Plovdiv, Tsanko Diustabanov St. 25, 4000 Plovdiv, Bulgaria.*

Keywords:

Cr-based hard coatings
Elasticity index
Resistance to plastic deformation
Resistance to crack formation

* Corresponding author:

Ekaterina Zlatareva
E-mail: ekpepe31@gmail.com

Received: 7 March 2023
Revised: 14 April 2023
Accepted: 13 May 2023

A B S T R A C T

Sets of Cr-based hard coatings were prepared via reactive closed field unbalanced magnetron sputtering (CFUBMS). Substrate temperature was kept in range of 150 to 200 ^{0}C during deposition. Nanohardness (H) and effective modulus of elasticity (E^*) of the coatings were examined, using depth-sensing indentation method. In order to present the mechanical properties and predict the tribological behaviour of the prepared coatings ratios H/E^* (elasticity index), H^3/E^{*2} (resistance to plastic deformation) and $1/(HE^{*2})$ (resistance to crack formation) were calculated and analysed. The results from the combined examination of the research ratios showed that they could be used for classification of the expected wear-resistant properties of Cr-based hard coatings deposited at temperature below 200 °C.

© 2023 Published by Faculty of Engineering

1. INTRODUCTION

The mechanical properties of materials are of interest in terms of their resistance to abrasive, erosive and impact wear. Wear resistance is usually believed to be relative to hardness and stiffness of hard ceramic materials. Although, significantly reflecting the resistance to plastic deformation, it is increasingly recognised that hardness is not necessary the main requirement for wear resistance [1]. Elasticity and toughness can be at least equally important factors [2]. Depending on the conditions of the mechanical process the material may show elastic, plastic or viscous properties, which combine in the various classes of materials [3]. Identifying these properties of the newly developed nanostructured materials is of great research interest.

Nowadays, mechanical components and tools are facing higher industrial performance requirements [1]. Deposition of hard coatings on machine components and tools made of conventional, structural and instrumental alloys is an effective method of improving their performance as economy is achieved and valuable natural resources are saved. Wear-, heat- and corrosion-resistant hard coatings steadily expand their various applications worldwide [4]. Cr-based coatings are widely applied on forming and cutting

tools, press stamps, parts for electrical machines, pneumatic and hydraulic devices [5,6]. Deposition temperature range below 200°C should meet the requirements of important contemporary heat sensitive industrial materials like cold working alloyed steels, copper alloys, die steels, polymers, etc. [7].

Magnetron sputtering has been applied for a long time as a flexible, reliable and effective method of physical vapour deposition of thin films [8]. Closed magnetic field, generated by unbalanced magnetrons in an arrangement whereby neighboring magnetrons are of opposite magnetic polarity, effectively increases plasma density and coating deposition rate as well as improves coating quality. This technology is popular as Close Filed Unbalanced Magnetron Sputtering (CFUBMS) [9]. Magnetron sputtering, allows deposition of different structures, satisfying a variety of property requirements through range of process parameters like substrate temperature, pressure, reactive gas flow, bias voltage, deposition time, etc. [4,10]. All of the above listed are subject to precise ongoing control during the complete technological process.

In general, the tribological behaviour of coatings is influenced by the contact conditions, environment conditions, contacting materials and composite coating/ substrate system [1].

Elastic behavior of ceramic coatings is usually represented by modulus of elasticity, which greatly influences stress distribution in coated elements. Load bearing capacity of coated elements increases with the increase in modulus of elasticity. Higher applied load is required to plastically deform substrate material, which is beneficial considering that coating will crack at the onset of plastic deformation of substrate material. Also, elastic modulus of the coating should match that of the substrate in order to avoid additional tensile stresses. Lower stress concentration is more significant than increased load bearing capacity for complete coating integrity. Large mismatch between elastic modulus of coating and substrate material leads to additional tensile stresses and is a prerequisite for compromising coating integrity. Proper values of the elastic modulus of the coating structures and their hardness should be achieved through variation of the coatings composition [11].

Hardness, effective Young's modulus and elastic recovery are currently used for presenting the mechanical behavior and prediction of tribological behavior of hard ceramic coatings. These parameters are easy to obtain via instrumented nanoindentation.

Ratios, which include hardness and elastic modulus like the ratio H/E^* (elasticity index), representing the capability of a coating to deform elastically without failure, H^3/E^{*2}, interpreting the resistance of a coating to plastic deformation and $1/(HE^{*2})$, related to crack formation, indicate the tribological behaviour of hard coatings. The focus of this research is prediction of tribological properties of Cr-based hard coatings, deposited via CFUBMS at low temperatures and intended for real industrial applications, which is based on the calculated ratios of H and E.

2. METHODOLOGY

Nanoindentation is a depth sensing method, appropriate for mechanical properties assessment of small ceramic samples or samples with very small thickness because of the application of very low loads [12]. Thus, mechanical properties of the coatings can be precisely determined since low loads allow that any influence of the substrate is avoided [13]. According to the thumb rule, the maximum penetration depth should be less than 10% of the total coating thickness in order that the influence of the substrate is eliminated. Some authors claim substrate independent measurements for penetrating depths up to 25% [14].

The hardness and the effective elastic modulus are calculated by applying the method, proposed by Oliver and Pharr, using indentation load/displacement curves [15], when the contact depth h_c is of small size and the imprint imaging is difficult. These curves visualise the data on the displacement of the indenter during loading and unloading. Usually linear mode of loading and unloading is applied for examination of ceramic materials.

Both elastic and plastic deformation occur during loading. A permanent impression is formed ought to plastic deformation and only elastic deformation is realised during unloading. These details in physical processes during indentation allow that hardness and elastic modulus are independently determined [14].

Oliver and Pharr define the hardness as the mean pressure the material supports under load [12]. The hardness is computed from

$$H = \frac{P_{max}}{A}, \quad (1)$$

where H – nanohardness, [GPa]; P_{max} – peak load, [mN]; A – projected area of contact at peak load, [nm^2].

During the nanoindentation elastic displacements occur both in the indenter and in the sample [15]. For any axisymmetric indenter a complex modulus of elasticity (reduced modulus) is determined from the analysis of load-displacement curves according to the relation:

$$E_r = \frac{\sqrt{\pi}}{2}\frac{S}{\beta\sqrt{A}}, \quad (2)$$

where: E_r – reduced modulus, [GPa]; S = dP/ dh – stiffness; A - projected area of contact at peak load, [nm^2] and geometry correction factor for a pyramid β = 1.034.

Reduced modulus is defined as follows:

$$\frac{1}{E_r} = \frac{(1-\nu^2)}{E} + \frac{(1-\nu_i^2)}{E_i}, \quad (3)$$

where: E_r - reduced modulus, [GPa]; E and E_i – Young's modulus for the specimen and the indenter, [GPa]; ν and ν_i – Poisson's ratio for the specimen and the indenter. For diamond indenter E_i = 1141 GPa and ν_i = 0.07.

Instrumented elastic modulus is calculated from (3):

$$E = \frac{(1-\nu^2)}{\frac{1}{E_r} - \frac{(1-\nu_i^2)}{E_i}}, \quad (4)$$

When the Poisson's ratio of the sample is unknown, an effective modulus can also be calculated:

$$E^* = \frac{1}{\frac{1}{E_r} - \frac{(1-\nu_i^2)}{E_i}}, \quad (5)$$

Determination of stiffness, contact depth and projected area is needed for the computing of coating's hardness and elastic modulus.

The procedure developed by Oliver and Pharr is based on the observation that unloading data are well described by a simple power law relation:

$$P = B(h - h_f)^m, \quad (6)$$

where the power-low constants B and m and the final displacement after removal of the indenter h_f are determined by a least squares fitting procedure. The initial unloading slope then corresponds to the experimentally measured contact stiffness: S = dP/dh of the upper portion of the unloading data and it is found by analytical differentiation and evaluation of the derivative at the peak load and displacement.

The area of contact at peak load is determined by the geometry of the indenter and the depth of contact after calibration of the area function with material of well-known module of elasticity. The area function describing the geometry of the indenter, relates the cross-sectional area of the indenter to the distance of its tip. It is assumed that the indenter itself does not deform significantly. For Berkovich indenter the area function is given by:

$$A_c = 24.56h_c^2 \quad (7)$$

The contact depth is determined from the experimental data according to the equation:

$$h_c = h_{\max} - h_s \quad (8)$$

where: h_c – contact depth, [nm]; h_{max} – peak displacement; h_s – displacement of the surface at the perimeter of the contact, [nm].

The deflection of the surface at the contact perimeter for a conical indenter according to Sneddon's expression is:

$$h_s = \frac{(\pi-2)}{\pi}(h - h_f) \quad (9)$$

Sneddon applied this solution only for the elastic component of the displacement. The force-displacement relation for the conical indenter is:

$$(h - h_f) = 2\frac{P}{S} \quad (10)$$

By substitution of this equation for contacting area at the maximal load there is obtained:

$$h_s = \varepsilon\frac{P_{\max}}{S}, \quad (11)$$

where: P_{max} - peak load, [mN]; h_s - displacement of the surface at the perimeter of the contact, [nm]; S - stiffness; ε - geometric constant (ε = 0.72 for Berkovich indenter).

Following this procedure of determination, the stiffness and area function and after that, instrumented elastic modulus and nanohardness could be calculated.

Leyland and Matthews investigated the ratio H/E as an indicator of coating durability [16]. They observed that even hard PVD coatings with low elastic modulus perform good wear resistance if their H/E ratio is high. Increasing the hardness and at the same time, keeping low values of elastic modulus is quite challenging for such coatings. Additionally, keeping the strain in the coating and in the substrate as close as possible, requires almost identical elastic modulus values of both for minimising the interfacial stress in the system and therefore the substrate could elastically deform with the coating without cracking or delamination. The achievement of higher H to E ratio reduces also the possibility of residual stress accumulation at the coating-substrate interface and the lower modulus of elasticity with values in the substrate modulus range benefit the coating itself. Attempts have been made that wear is correlated to the H/E ratio of the hard coatings, as predicting the H/E ratio for PVD hard coatings could show their potential to resist the substrate strain, indicating their wear-resistant properties [17]. In contact mechanics theory for flat surface in elastic/plastic contact with a rigid ball of radius R there is shown that yield pressure P_y is a function of the ratio H^3/E^2 through the equation [18]:

$$P_y = 0.78R^2(H^3/E^2) \quad (12)$$

During the development of Instrumented indentation theory, it is accepted that the load-displacement curve before the appearance of a pop-in is fully reversible and the Hertzian contact theory could be interpreted [19]. The difference of induced stress when sharp and blunt indenter are used is consistent with the influence of the nanoindentation size effect. It is researched that for sufficiently small indents, the material in the highly stressed zone underneath the indenter is without dislocations and if the indenter radius increases, it is more likely a nearby dislocation to assist the plasticity deformations. The estimated Hertzian radii are found to be 163 nm for a sharp Berkovich indenter and over 1 micron for a blunt indenter [19]. The fabricated new Berkovich indenters are having rounded spherical type indenter tip with radius between 50-100 nm [20]. When R/h_{max} is over 6.4 for elastic contact and over 2 for elastic-plastic contact the geometry of the blunt Berkovich indenter with tip end radius R behaves as a spherical one [21]. The indentation size effect due to the yield stress also depends mainly on the size of the contact area and is independent of the indenter geometry [22]. Following this data when nanoindentation is done at shadow depths the Py also will follow the spherical part of the Berkovich indenter with prevailing elastic deformation and we could accept the relation in equation (12) is valid also for Berkovich indenters as it is made by Tsui, Pharr and Oliver [23]. When deeper nanoindentation is done the sharper pyramidal geometry will determine the contact area but the shape of the plastic zone will still follow the spherical tip defect of the Berkovich indenter. Then it is supposed that Py will also be in relation with the ratio H^3/E^{*2} and it could be used for estimation of the resistance to plastic deformations. The geometry of Berkovich indenter is widely used for identifying the load carrying capacity of hard coatings on softer substrates [16].

For surfaces with higher H^3/E^2 at given contact pressure the contact is seen to be elastic and this ratio is accepted to be considered as a measure of the resistance to plastic deformation or load-carrying capacity of a material. For the system coating/substrate this property is more complex because of the dependence of the initial point of yielding and forward fatigue behaviour.

As the ratio H/E is a measure of the elastic strain limit and the ratio H^3/E^2 defines the limit of plastic deformation, both could be associated to toughness properties of hard coatings [24]. To estimate the fracture toughness of coatings, more complex measurements are required. Both ratios with more easily obtained H and E values are a good alternative to predict this property. The authors claim that these ratios are only good for coatings with fractures, leading to instant failure. For nanocomposite and nanolayered coatings, where the interfaces stop the propagation of the cracks the estimation of the coating toughness through H/E and H^3/E^2 is not generally advisable [24].

The nanohardness and effective elastic modulus of a coating can be controlled through its chemical composition, i.e. the parameters of deposition process. Thus coatings with desired mechanical properties can be obtained for specific applications [25].

The ratio $1/(HE^2)$ is also used for characterisation of Cr-based hard coatings, deposited via CFUBMS, for indication of crack formation. Greater ratio shows resistance to crack formation, and titanium content in CrTiN coatings significantly influences this property [26].

Young's modulus is used for modelling wear resistance in coating applications taking part in Archard's equation and in empirical relation between wear and the mechanical properties. Reduced modulus E_r is also used in different nanohardness to elastic modulus ratios like H/E, $(H/E)^2$, $H^2/2E$, H/E_r^2 and H^3/E^2 as indicators for abrasion resistance of rigid-plastic materials [27].

As we could see, achieving a combination of high values of hardness and low values of module of elasticity could significantly reduce the possibilities of crack formation. Thus, the fracture toughness and cutting efficiency of hard coatings, deposited on industrial substrates, could be predicted. In some cases, it is more important that industrial hard coatings have optimal ratios H to E than achieving of extremely high hardness [16]. The analysis of the results, obtained via instrumented indentation testing of nanohardness and effective modulus of elasticity at penetration depths under 25% of the coating thickness could be used for improving the mechanical properties of Cr-based hard coatings and predicting their wear resistance.

3. EXPERIMENTAL DETAILS

All of the coatings were deposited onto hardened high-speed steel (HSS) substrates via CFUBMS. The steel type is P6M5 (chemical composition: 0.84% C; 5.96% W;4.96% Mo; 3.99% Cr; 1.94% V, 0.25% Si, 0.27% Mn, 0.024% P, 0.005% S, 0.38 Ni, 0.16 V) produced by Zaporizhstal, OAO Zaporozhye Metallurgical Plant in Ukraine. This type of HSS steel could be used for different applications [28].

The process was carried out on UDP 850 system (Teer Coatings Ltd), equipped with four rectangular magnetrons. Two oppositely faced Ti targets, a Cr target and an Al target, all of them of high purity (99,999 %), were used. DC current was applied to the Ti and Cr targets and pulsed current (150 kHz, 1500 ns) was applied to the Al target. The substrates were degreased in a commercial cleaning solution, ultrasonically cleaned, rinsed in distilled water and dried prior to the deposition process. The base pressure of the vacuum chamber was brought to below $3.3x10^{-3}$ Pa and the working pressure was maintained at 0.20 Pa. Gas flow of both, the inert gas (Ar) and the reactive gas (N_2) were controlled by mass flow controllers. The rate of the samples holder was kept at 5 rpm. Prior to deposition the samples were cleaned in Ar plasma for 30 minutes at a bias voltage of -500 V for removing contaminants from the substrate surface. Bias voltage of -70 V was applied to the samples and the substrate temperature was in diapason of 150 to 200 ^{0}C during all of the deposition processes.

In order to improve the adhesion to the substrate and to lower the inner stress, initially a Cr adhesive layer (~ 0.1 μm) was deposited onto the substrate, applying DC current of 6A to the chrome target. Then a CrN buffer layer (~ 0.2μm) was deposited. The transition layer was deposited via parallel gradient of nitrogen flow and metal sputtered material.

After optimization of the technological regimes nine Cr-based coatings were deposited below 200 °Cwith different ratio of contained metals and nitrogen: Cr, CrN, CrAlN, CrTiN and CrTiAlN. These Cr-based coatings were chosen as they are developed for different industrial applications, requiring deposition as an individual coating, an adhesion and transition layer or in a multilayer structure. Consequently, the thickness D of the obtained coatings was in the range of 0.7 μm to 2.6 μm.

The chemical composition of the coatings was controlled by varying the current of the targets in range of 4 to 8A and the nitrogen gas flow in range of 15 to 30 sccm.

Samples with Cr-based layers, deposited with different composition and thicknesses, allow their mechanical properties to be examined and classified depending on the materials used.

The mechanical properties of the coatings were characterised via depth sensing method. A Nanoindentation Hardness Tester (NHT) (Anton Paar), equipped with a diamond Berkovich indenter was used. The applied load was in range of 10 to 20 mN and the mechanical properties of the coatings were precisely determined since low

loads allowed any influence of the substrate to be avoided. By decreasing the indentation depth, the so-called indentation Size Effect (ISE) appears. There are different reasons for the existence of ISE like imperfections in the indenter, surface roughness, leading to alteration of the contact radius, different asperities under the indenter, groove or convex contact, etc. [29]. The influence of ISE could be reduced with decreasing the ratio h/δ, where h is indentation depth and δ is the surface roughness [29]. The Cr based coatings of this class normally have roughness around 20 nm [30]. Indentation depths lower than 10% of the coating thickness are not recommended because they will lead to an increase in the ISE effect and corresponding error in the measurements. The substrate surfaces are also characterized with waviness that is followed by the deposited coating. To avoid the influence of the waviness a depth adjustment is made before each measurement and the place of the indentation is appropriately chosen for each sample. The hardness and the elastic modulus were calculated, applying the method, proposed by Oliver and Pharr.

The deposition parameters are summarized in Table 1.

Table 1. Technological parameters.

#	I_{Al}, [A]	I_{Ti}, [A]	I_{Cr}, [A]	N_2, [sccm]	N_2/Ar	p, [mTorr]	t, [min]	D, [μm]
Cr	-	-	6.0	-	-	1.4	120	1.42
CrN	0.5	0.5	6.0	16.3	0.604	1.7	120	1.75
CrAlN(1)	4.0	0.5	8.0	19.7	0.788	1.6	180	2.50
CrAlN(2)	8.0	-	4.0	15.0	0.833	1.5	80	0.70
CrTiN(1)	0.5	8.0	6.0	20.0	0.800	1.5	150	2.60
CrTiN(2)	0.5	8.0	4.0	19.6	0.784	2.0	180	1.50
CrTiAlN(1)	6.0	8.0	4.0	30.0	1.200	2.7	120	1.00
CrTiAlN(2)	6.0	6.0	6.0	26.0	1.040	2.4	180	1.68
CrTiAlN(3)	4.0	6.0	4.0	22.0	0.880	2.2	180	1.60

4.RESULTS AND DISCUSSION

The calculated values of nanohardness (H) and effective elastic modulus (E*) are shown in Table 2. The corresponding H to E^* ratios, related to elasticity index (H/E^*), resistance to plastic deformation (H^3/E^{*2}) and crack formation ($1/(H.E^{*2})$) are presented in Table 2 too.

Table 2. Mechanical properties of the substrate and the coatings.

#	Coating	H, [GPa]	E*, [GPa]	H/ E*	H^3/E^{*2}, [GPa]	$1/(H.E^{*2})$, 10^{-7}, [GPa^{-3}]
1	Cr	8.1	295	0.0275	0.0061	14.1864
2	CrN	17.9	383	0.0467	0.0391	3.8085
3	CrAlN(1)	19.1	368	0.0519	0.0515	3.8661
4	CrAlN(2)	20.1	279	0.0720	0.1043	6.3914
5	CrTiN(1)	27.4	272	0.1007	0.2780	4.9330
6	CrTiN(2)	29.9	392	0.0763	0.1740	2.1765
7	CrTiAlN(1)	39.1	374	0.1045	0.4274	1.8284
8	CrTiAlN(2)	32.4	399	0.0812	0.2136	1.9387
9	CrTiAlN(3)	30.5	358	0.0852	0.2214	2.5582
10	HSS	11.5	274	0.0420	0.0203	11.5825

Fig. 1(a) and Fig. 1(b) show load/ displacement curves of bare substrate (HSS) and of all of the samples. Load of 200 mN was used for nanoindentation testing of the substrate, considered as bulk material. The coating mechanical properties were examined by the application of different load, chosen in the range of 10 to 20 mN for each sample depending on its thickness. This differentiation of loads guarantees indentation depth of less than 25% of each coating thickness and decreasing the substrate and ISE effects.

All the curves seemed typical for the examined systems substrate-coating. Any significant unevenness and discontinuities were not

detected here, as no cracks occurred at these load values. An increased slope of coatings curves' loading part and smaller residual depth were observed compared to the bare substrate. That was caused by slower penetration of the indenter into the material. All of these show improved mechanical properties of the coatings, compared to HSS substrate.

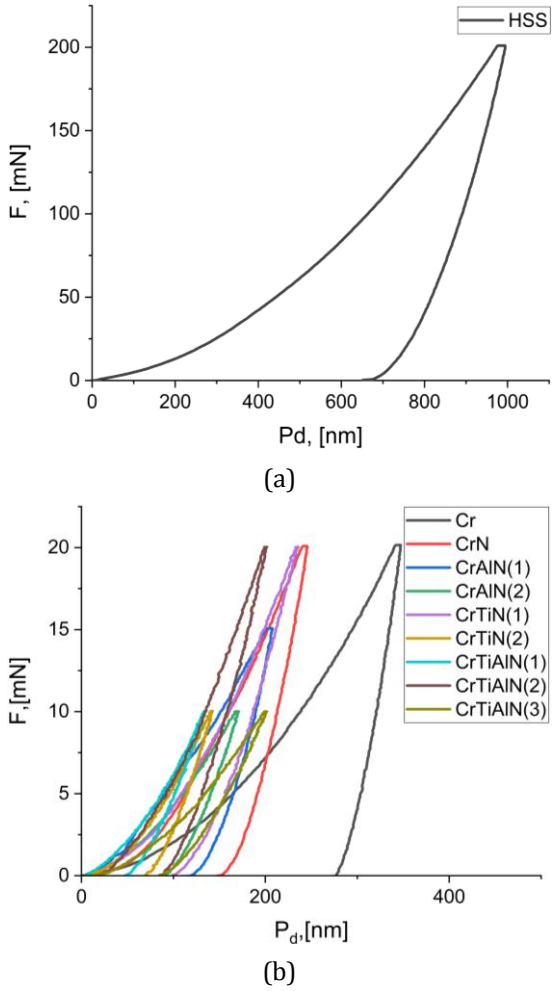

Fig. 1. Load/ displacement curves: (a) of HSS; (b) of the coatings.

Fig. 2 presents hardness and effective modulus of elasticity of the examined coatings and of the bare substrate. The results reveal complex correlation between the values of these parameters.

Literature data for Cr coatings show nanohardness value in range of 11-14 GPa. Depending on the nitrogen content in CrN layers the nanohardness could vary from that of Cr and to 28 GPa. High hardness comes out mainly from the presence of the harder nitride phase and not from an internal stress [31,32].

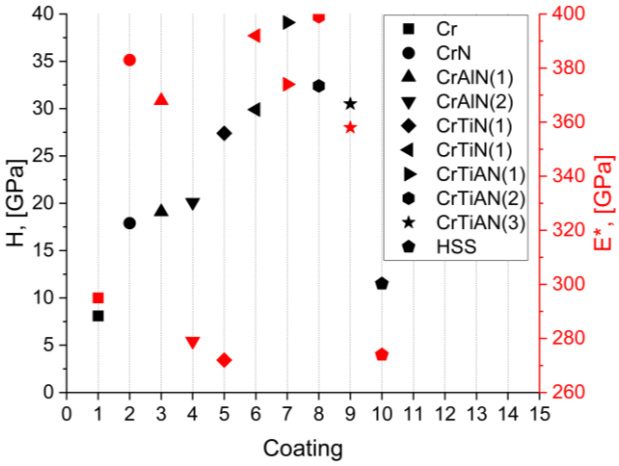

Fig. 2. Nanohardness and modulus of elasticity.

For these coatings the higher values of nanohardness are found for compositions, consisting of Cr, Cr_2N and CrN phases [33]. For CrN based coatings the typical nanohardness is 18 GPa. As TiN shows nanohardness of more than 20 GPa and Al could form metastable phase with CrN, both Ti and Al are added to CrN layers for increasing their nanohardness [34]. Depending on the deposition conditions the nanohardness of CrAlN coatings could be also in a wide diapason: 15-36 GPa [35]. The reported values for CrTiN coatings are between 25-29 GPa and for CrTiAlN - to 35 GPa [26]. As expected, the examination of the deposited ternary and quaternary coatings showed higher values of hardness than Cr (8 GPa) and CrN ones (18 GPa). The nanohardness of CrAlN was in range of 19-20 GPa, for CrTiN it was between 27-30 GPa and for CrTiAlN - between 30-39 GPa.

The results show that some of the coatings have higher nanohardness although they are deposited with lower thickness. Assuming that the substrate influence is minimal we compare the mechanical properties depending on the deposited coating materials.

Compared to each other, coatings of the same element content, deposited under different process conditions (target current, nitrogen flow, working pressure), revealed some dissimilarity in their mechanical properties. Close values of hardness, but quite different values of effective modulus of elasticity were obtained. As a rule, with the increase of the harder phases content the module of elasticity also increases. The measured values of

modulus of elasticity for the different layers are as follows: Cr (300 GPa), CrN (380 GPa), CrAlN (280-370 GPa), CrTiN (270-390 GPa) and CrTiAlN (360-400 GPa). One of the reasons for the variation of the values of module of elasticity is the dependence of the mechanical properties on the nitrogen content [36]. Hard coatings with similar hardness could also have a different modulus of elasticity because of variation in their chemical composition [37]. As a conclusion, the nanohardness and modulus of elasticity are improved for the ternary and quaternary Cr-based coatings by comparison with the substrate and the binary CrN coatings. The variation of H and E in dependence on the composition and structure leads to obtaining of different H to E ratios and they could be used for establishment of the optimal deposition conditions, corresponding to the improved tribological and fracture resistance properties.

Ratios H/E^* and H^3/E^{*2} in function of nanohardness could be examined [11]. Fig. 3 presents plots of the H/E^*, H^3/E^{*2} and $1/(H.E^{*2})$ ratios in dependence on nanohardness of the investigated coatings. It is seen that higher nanohardness does not correspond to higher resistance to wear for CrTiN and CrTiAlN coatings. All the coatings, except the chromium one, showed improved characteristics compared to the substrate itself.

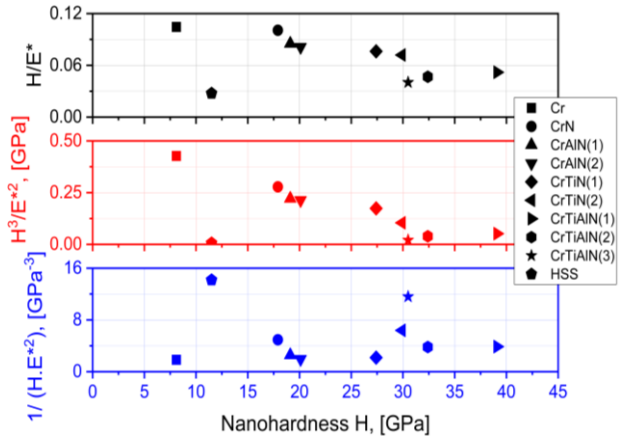

Fig. 3. H/E^*, H^3/E^{*2} and $1/(H.E^{*2})$ in dependence on nanohardness.

Because of their different ranges of variation of the effective modulus of elasticity, and a little, but essential difference in nanohardness, ternary and quaternary coatings with similar deposition structure showed indices of resistance to wear and to plastic deformation varying significantly. As the elastic modulus values vary in a wide diapason, depending on the deposition method and process conditions, the H to E ratios found in literature for the researched coatings are in a wide diapason. For example, H/E for CrN coating is estimated from 0.021 to 0.079 [38].

Deposited as stoichiometric interlayer CrN shows H/E value of 0.071 [39]. For CrAlN layers higher value of H/E – 0.089 is found [40]. CrAlN coating with CrAl transition layer is characterized by H/E in the range of 0.097-0.123 and by H^3/E^2 in range of 0.333-0.394 [41]. Literature values for both ratios for CrN, CrAlN, CrTiN and CrTiAlN coatings measured by Wang at all are presented in Table 3 [42].

Table 3. H/E and H^3/E^2 values measured by Wang at all [42].

Coating	H/E, -	H^3/E^2, [GPa]
CrN	0.054	0.042
CrTiN	0.047	0.031
CrAlN	0.056	0.056
CrTiAlN	0.068	0.1030

It is obvious from the literature results, that both ratios increase their values with the complication of the coating structure.

The $1/(HE^{*2})$ ratio values are also fluctuating in dependence on the nanohardness and the used materials. High values of this index predict better resistance to crack formation. The HSS substrate is characterised by a $1/(HE^{*2})$ ratio close to this of the Cr layer and so the last one is appropriate to be used as first adhesion layer. The deposited CrN layer shows intermediate $1/(HE^{*2})$ ratio values between these of Cr and the other complicated structures, and it could be used as a transition layer, reducing stress and the possibilities for crack initiation in the coatings. The low values of this ratio for the ternary CrTiN and quaternary coatings could be explained with the Ti content in their composition. Thus titanium increases their hardness, but also makes them brittle and lowers their resistance to crack formation [43]. The Cr to Ti ratio in these structures could also influence the crack formation mechanisms [44].

The different ratio analysis reveals that CrTiN and CrTiAlN coatings showed high values of H/E and H^3/E^{*2} and low values of 1/ (HE^{*2}). The Cr coating and the substrate itself showed very low values of the ratios H/E and H^3/E^{*2} in combination with high values of 1/ (HE^{*2}). CrAlN and CrN coatings were characterised by close intermediate values of H/E*, H^3/E^{*2} and 1/ (HE^{*2}). Following this analysis, we could classify the examined Cr-based coatings in three groups presented in Fig. 4.

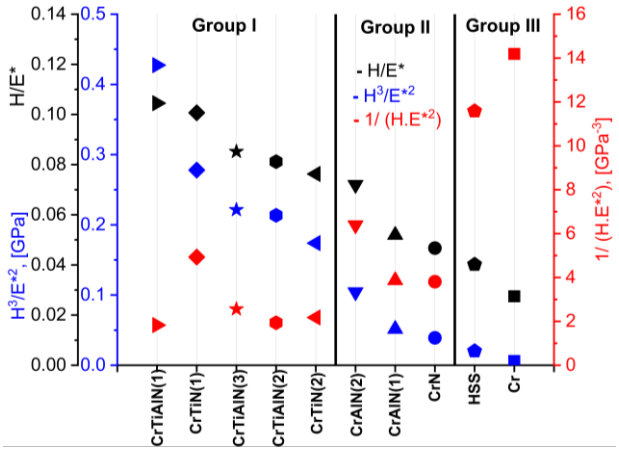

Fig. 4. Groups according to H/E*, H^3/E^{*2} and 1/(HE^{*2}) ratios.

The samples in group III with their properties are out of interest for this examination and could be used only for comparison with the other two groups. The coatings from group II have intermediate wear-resistance and toughness properties and it is supposed that they could be applied on tools working in not so heavy industrial conditions.

Both CrTiAlN and CrTiN coatings structures, forming group I are expected to have good wear-resistant properties, when deposited on the base of a Cr adhesion layer and a CrN transition layer. Superior combination of properties could be expected for some of the CrTiN coating structures with regard to the values of all of the examined magnitudes. As seen in *Table 2*, at a relatively high hardness (27.4 GPa), but still lower than this of CrTiN(2) and CrTiAlN coatings, CrTiN(1) one was characterised by the lowest modulus of elasticity of all the examined coatings. Its effective modulus of elasticity matched best this of the substrate itself. Group one's CrTiN (1) coating was characterised by relatively well-balanced values of H/E*, H^3/E^{*2} and 1/(HE^{*2}) ratios.

4. CONCLUSIONS

- Several sets of Cr-based hard coatings were prepared using closed field unbalanced magnetron sputtering. Their nanohardness and effective modulus of elasticity were determined via nanoindentation testing.
- Ratios H/E*, H^3/E^{*2} and 1/(HE^2), relative to nanohardness and elastic modulus were calculated and their values were compared. Some promising results were reported in this work.
- The mechanical properties of the ternary and quaternary coatings were improved, compared to these of bare substrate, chromium and chromium nitride.
- The coatings were divided into groups according to these ratios and suppose to their potential application.
- Intermixing of ranges of the examined ratios for CrTiAlN and CrTiN coatings were identified. We assume that both types of coatings could be developed for different industry applications. CrTiAlN coatings could be preferred because of their high hardness and resistance to plastic deformation, and CrTiN coatings - when high toughness and resistance to cracks are demanded.

The results from the combined examination of the ratios H/E*, H^3/E^{*2} and 1/(HE^2) showed that they could be used for classification of the presumed wear-resistant properties of Cr-based coatings, deposited at temperature below 200°C, and for optimisation of the technological processes of their deposition. The forward examination step requires execution of real tribological tests in order to validate this preliminary classification.

Acknowledgements

This work was supported by the European Regional Development Fund within the OP "Science and Education for Smart Growth 2014 – 2020", Project CoC "Smart Mechatronic, Eco- and Energy Saving Systems and Technologies", № BG05M2OP001-1.002-0023.

REFERENCES

[1] K. Holmberg, A. Matthews, *Coatings Tribology: Properties, Mechanisms, Techniques and Applications in Surface Engineering*, 2nd edition, Elsevierv Science 2009.

[2] A. Layland, A. Mattews, *On the significance of the H/E ratio in wear control: a nanocomposite coating approach to optimised tribological behaviour*, Wear, vol. 246, iss. 1-2 pp. 1-11, 2000, doi: 10.1016/S0043-1648(00)00488-9

[3] A. Baltov, M. Popova, *Material mechanics*, Academic Publishing "Prof. Marin Drinov", 2009.

[4] M. Ilieva, *Obtaining and investigation of hard, wear-resistant protective chrome-based coatings*, PhD Thesis, Angel Kanchev University of Rousse, Rousse, 2011

[5] B. Navinšek, *Industrial application of CrN (PVD) coatings, deposited at high and low temperatures*, Surface and Coatings Technology, vol. 97, iss. 1-3, pp. 182-191, 1997, doi: 10.1016/S0257-8972(97)00393-9

[6] S.M. Aouadi, D.M. Schulze, *Growth and characterization of Cr_2N/ CrN multilayer coatings*, Surface and Coatings Technology, vol. 140, iss. 3, pp. 269-277, 2001, doi: 10.1016/S0257-8972(01)01121-5

[7] D. Doudlas, *Lower Deposition Temperature PVD Coatings Allow for Greater Choice in Mold Materials*, MoldMaking Technology, 2008, available at: https://www.moldmakingtechnology.com/articles/lower-deposition-temperature-pvd-coatings-allow-for-greater-choice-in-mold-materials

[8] J.T. Gudmundsson, *Physics and technology of magnetron sputtering discharges*, Plasma Sources Science and Technology, vol. 29, no. 11, 2020, doi: 10.1088/1361-6595/abb7bd

[9] Y. Deng, C. Wanglin, *Physical vapour deposition technology for coated cutting tools: A review*, Ceramics International, vol. 46, iss. 11, pp. 18373-18390, 2020, doi: 10.1016/j.ceramint.2020.04.168

[10] E. Alfonso, J.Olaya, G. Cubillos, *Thin Film Growth Through Sputtering Technique and Its Applications*, Ch.15 in M.R.B. Andreeta (Ed.): Crystallization – Science and Technology, IntechOpen, pp. 424-428, 2012, doi: 10.5772/35844

[11] A. Miletić, P. Panjan, M. Cekada, *Elastic-plastic behaviour of hard coatings*, Journal for Technology of Plasticity, vol. 42, no. 2, 2017, doi: 10.24867/jtp.2017.42-2.11-22

[12] H. Xiao, *Theoretical model for determining elastic modulus of ceramic materials by nanoindentation*, Materialia, vol. 17, 2021, doi: 10.1016/j.mtla.2021.101121

[13] W.C. Oliver, G.M. Pharr, *An improved technique for determining hardness and elastic modulus using load and displacement sensing indentation experiments*, Journal of Material Research, vol. 7, pp. 1564–1583, 1992, doi: 10.1557/JMR.1992.1564

[14] G.M. Pharr, W.C. Oliver, *Measurement of Thin Film Mechanical Properties, Using Nanoindentation*, MRS Bulletin, vol.17, iss.7, pp. 28-33, 1992, doi: 10.1557/S0883769400041634

[15] W.C. Oliver, G.M. Pharr, *Measurement of hardness and elastic modulus by instrumented indentation: Advances in understanding and refinements to methodology*, Journal of Material Research, vol. 19, pp. 3-20, 2004, http://dx.doi.org/10.1557/jmr.2004.0002

[16] B. Beake, *The influence of the H/E ratio on wear resistance of coating systems -Insights from small-scale testing*, Surface and coatings technology, vol. 442, 2022, doi: 10.1016/j.surfcoat.2022.128272

[17] S. Shafiel, M. Divandari, S.M. Ali Boutorabi, *Evaluation of modulus of elasticity, nanohardness and stiffness of TiCN coating deposited by PACVD*, Technium, vol. 2, no. 4, pp. 33-38, 2020, doi: 10.47577/technium.v2i4.770

[18] B. Beake, *Nano- and Micro-Scale Impact Testing of Hard Coatings: A Review*, Coatings, vol. 12, iss. 793, 2022, doi: 10.3390/coatings12060793

[19] L. Ma, L. Levine, R. Dixson, D. Smith, D. Bahr, *Effect of the spherical indenter tip assumption on the initial plastic yield stress,* in J. Nemecek (Ed.): Nanoindentation in material science, IntechOpen, 2012, doi: 10.5772/48106

[20] A. C. Fischer-Cripps, *Introduction to contact mechanics*, Springers, 2000, doi: 10.1007/b97709

[21] K. Jha, Sh. Zhang, N. Suksawang, T. Wang, A. Agarwal, *Work-of-indentation as a means to characterize indenter geometry and load-displacement response of a material*, Journal of Physics D: Applied Physics, vol. 46, 2013, doi: 10.1088/0022-3727/46/41/415501

[22] A. Bushby, T. Zhu, D. Dunstan, *Slip distance model for the indentation size effect at the initiation of plasticity in ceramics and metals,* Journal of materials research, vol. 24, iss. 3, doi: 10.1557/jmr.2009.0104

[23] T.Y. Tsui, G.M. Pharr, W. Oliver, C.S. Bhatia, R.L. White, S. Anders, A. Anders, I.G. Brown, *Nanoindentation and Nanoscratching of Hard Carbon Coatings for Magnetic Disk,* Materials Research Society symposia proceedings, vol. 383, pp. 447-452, 1995, doi: 10.1557/PROC-383-447

[24] X. Chen, Y. Du, Y. Chung, *Commentary on using H/E and H3/E2 as proxies for fracture toughness of hard coatings*, Thin Solid Films, vol. 688, 2019, doi: 10.1016/j.tsf.2019.04.040

[25] *Handbook on instrumented indentation*, CSM Instruments SA, 2008

[26] M. Sharear Kabir, P. Munroe, *Structure and mechanical properties of graded Cr/CrN/CrTiN coatings synthesized by close field unbalanced magnetron sputtering*, Surface and Coatings Technology, vol. 309, pp. 779-789, 2017, doi: 10.1016/j.surfcoat.2016.10.087

[27] G. Pintaude, *Introduction of the ratio of the hardness to the reduced elastic modulus for abrasion*, Ch. 7, in J. Gegner (Ed.): Tribology-fundamentals and advancements, IntechOpen, pp. 217-230, 2013, doi: 10.5772/55470

[28] A. Adaskin, *Applicability of P6M5 steel*, Russian engineering research, vol. 30, no.2 pp. 186-189, 2010, doi: 10.3103/S1068798X10020206

[29] X. Li, W. Zhang, M. Ham, F. Xie, D. Li, J. Zhang, B. Long, *Indentation size effect: an improved mechanistic model incorporating surface undulation and indenter tip irregularity,* Journal of materials research and technology, vol. 23, p. 143-153, 2023, doi: 10.1016/j.jmrt.2023.01.001

[30] M. Kabir, P. Munroe, Z. Zhou, Z. Xie, *Scratch adhesion and tribological behaviour of graded Cr/CrN/CrTiN coatings synthesized by closed-field unbalanced magnetron sputtering,* Wear, vol. 380-381, pp. 163-175, 2017, doi: 10.1016/j.wear.2017.03.020

[31] P. Hviščová, F. Lofaj, M. Novak, *Nanohardness of CrN coatings versus deposition parameters*, Key Engineering Materials, vol. 606, pp. 191-194, 2014, doi: 10.4028/www.scientific.net/KEM.606.191

[32] P. Hviščová, F. Lofaj, M. Novak, *The influence of deposition conditions on the nanohardness and scratch behaviour of thin DC magnetron sputtered CrN coatings*, Powder Metallurgy Progress, vol. 13, no 3-4, pp. 175-178, 2013, doi: 10.4028/www.scientific.net/KEM.606.175

[33] A. Vyas, Z. Zhou, *Sputter deposited nanocomposite Cr-based films and their characterization*, in M. Ceccarelli (Ed.): Mechanisms and machine science, Springer, pp. 245-255, doi: 10.1007/978-3-030-67958-3_27

[34] E. Mohammadpour, Z-T. Jiang, M. Altarawneh, Z. Xie, Z-f Zhou, N. Mondinos, J. Kimpton, B. Dlugogorski, *Estimation of high temperature mechanical properties of CrN and CrAlN coatings from in-situ Synchrotron radiation X-ray diffraction*, in Asia Oceania forum for synchrotron radiation research, 25-27 November, 2015, National centre for synchrotron science.

[35] Y. Benlatreche, C. Nouveau, H. Aknouche, L. Imhoff, N. Martin, J. Gavoille, C. Rousselot, J.-Y. Rauch, D. Pilloud, *Physical and mechanical properties of CrAlN and CrSiN ternary systems for wood machining applications*, Plasma Processes and Polymers, vol. 6, iss. S1, pp. S113-S117, 2009, doi: 10.1002/ppap.200930407

[36] J. Sullivan, F. Huang, J. Barnard, M. Weaver, *Effect of nitrogen pressure on the hardness and chemical states of TiALCrN coatings*, Journal of vacuum science & technology A, vol. 23, iss. 1, pp. 78-84, 2005, http://dx.doi.org/10.1116/1.1830498

[37] J. Musil, F. Kunc, H. Zeman, *Relationships between hardness, Young's modulus and elastic recovery in hard nanocomposite coatings*, Surface and Coatings Technology, vol. 154, iss. 2-3, pp. 304-313, 2002, doi: 10.1016/S0257-8972(01)01714-5

[38] H. Kim, J. La, K. Kim, S. Lee, *The effects of the H/E ratio of various Cr-N interlayers on the adhesion strength of CrZrN coatings on tungsten carbide substrates*, Surface and Coatings Technology, vol. 284, pp. 230-234, 2015, doi: 10.1016/j.surfcoat.2015.06.077

[39] H. Kim, S. Kim, S. Lee, *Mechanical properties and thermal stability of CrZrN/CrZrSiN multilayer coatings with different bilayer periods*, Coatings, vol. 12. iss. 7, 2022, doi: 10.3390/coatings12071025

[40] H. Kim, S. Kim, S. Lee, *Influence of interlayer materials on the mechanical properties and thermal stability of a CrAlN coating on a tungsten carbide substrate*, Coatings, vol. 12, iss. 8, 2022, doi: 10.3390/coatings12081134

[41] L. Liu, Q. Ruan, Z. Wu, D. Li, C. Huang, Y. Wu, T. Li, Z. Wu, X. Tian, R. Fu, P. Chu, *Fabrication and cutting performance of CrAlN/CrAl multilayer coatings deposited by continuous high-power magnetron sputtering*, Ceramica international, vol. 48, iss. 10, pp. 14528-14536, 2022, doi: 10.1016/j.ceramint.2022.01.346

[42] Q. Wang, F. Zhou, J. Yan, *Evaluating mechanical properties and crack resistance of CrN, CrTiN, CrAlN and CrTiAlN coatings by nanoindentation and scratch tests*, Surface and Coatings technology, vol. 285, pp. 203-213, 2016, doi: 10.1016/j.surfcoat.2015.11.040

[43] A. Vereschaka, S. Grigoriev, A. Chigarev, F. milovich, N. Sitnikov, N. Andreev, C. Sotova, J. Bublikov, *Development of a model of crack propagation in multilayer hard coatings under conditions of stochastic force impact*, Materials, vol. 14, iss. 2, 2021, doi: 10.3390/ma14020260

[44] X. Zeng, S. Zhang, J. Hsieh, *Development of graded Cr-Ti-N coatings,* Surface and coatings technology, vol. 102, iss. 1-2, pp. 108-112, 1998, doi: 10.1016/S0257-8972(97)00682-8